

Self-Supervised Learning for Joint Pushing and Grasping Policies in Highly Cluttered Environments

Kamal Mokhtar¹, Cock Heemskerk², Hamidreza Kasaei¹

Abstract—Robots often face situations where grasping a goal object is desirable but not feasible due to other present objects preventing the grasp action. We present a deep Reinforcement Learning approach to learn grasping and pushing policies for manipulating a goal object in highly cluttered environments to address this problem. In particular, a dual Reinforcement Learning model approach is proposed, which presents high resilience in handling complicated scenes, reaching an average of 98% task completion using primitive objects in a simulation environment. To evaluate the performance of the proposed approach, we performed two extensive sets of experiments in packed objects and a pile of object scenarios with a total of 1000 test runs in simulation. Experimental results showed that the proposed method worked very well in both scenarios and outperformed the recent state-of-the-art approaches. Demo video, trained models, and source code for the results reproducibility purpose are publicly available. <https://github.com/Kamalnl92/Self-Supervised-Learning-for-pushing-and-grasping>.

I. INTRODUCTION

Grasping is a crucial skill for many robotics applications. It enables robots to perform numerous tasks, which are otherwise impossible without a versed object’s grasp. It further opens opportunities to robots to numerous skills that are not attainable without a versed object’s grasp. In many scenarios, objects do not appear in isolation, and therefore, grasping a target object might not be feasible due to occlusion and cluttered presence in the environment. Inspired by human dexterity, a robot should have a set of primitive motions such as pushing to single out the target object from the clutter and make future grasp feasible. Such a sequence of actions by a robot is depicted in Fig. 1. In order to reach this level of reasoning, the robot must consider the visual observation of the goal object(s) and emphasize the spatial equivalence to reach a successful grasp. In other words, object grasping is not a simple antipodal grasp action. It requires a cohesive system that all operate in harmony resulting in a smooth action. Starting from the sensory information of the robot acquired from its surrounding environment, which could have flaws, the robot needs to handle such circumstances. Additionally, the scene can change dynamically after each action and before a task is completed, which requires the robot’s resilience. Furthermore, the motion planning of a robotic arm to get into the desired pose is challenging in itself. Therefore, the robot needs to observe the environment and adapt accordingly constantly [1].

¹Department of Artificial Intelligence, Bernoulli Institute, University of Groningen, 9747 AG, The Netherlands.

² Heemskerk Innovative Technology, Delft, The Netherlands
email: mokhtar.kamal@icloud.com, hamidreza.kasaei@rug.nl

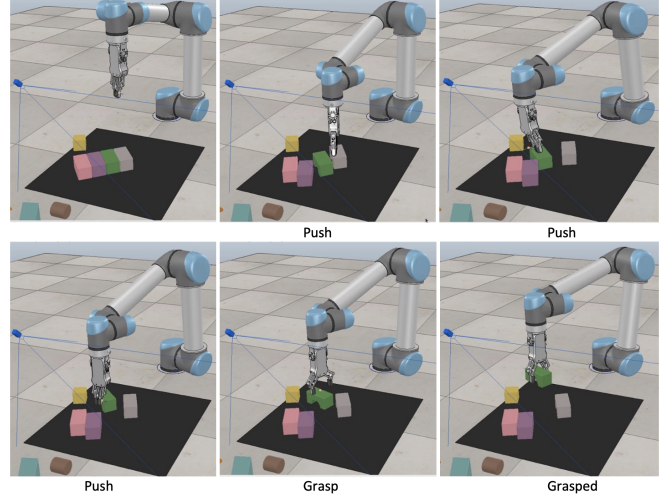


Fig. 1. Infeasible grasp action as a result of densely packed blocks, requiring pre-manipulation push actions. In this example, the target object, shown in green, is not graspable due to other objects present; the robot pushes the target object in a way to make it graspable. Eventually, the robot grasps the object successfully.

This paper mainly focuses on self-supervised learning for pushing and grasping objects in highly cluttered environments via deep Reinforcement Learning (RL). There has been number of study’s evolving around the concept of the synergy between pushing and grasping, i.e., primitive motion push to grasp [2] [3] [4] [5] [6] [7] [8]. However, most of the previous work is intended for bin picking, emptying objects from one bin, and dropping them in another. In this work, we exploit scenarios where the goal object is initially not graspable due to surrounding clutter. The synergy between pushing and grasping flourishes the coherent behavior between pushing and grasping. Unlike having any models working independently from the other, which often result in unpredictable changes in the scene and strain in solving the issue, we propose a deep RL approach to exploit the potentials and limitations of the synergy between pushing and grasping. The overall system architecture, which will be discussed in more detail in section III is demonstrated in Fig. 2. In summary, our contributions are threefold:

- We develop a self-supervised learning approach for a service robot to jointly learn push and grasp policies to clear occlusion around goal objects. We train the model for more challenging tasks, namely grasping and removing obstacles; exploring model and system limitations.
- We perform extensive sets of experiments to evaluate

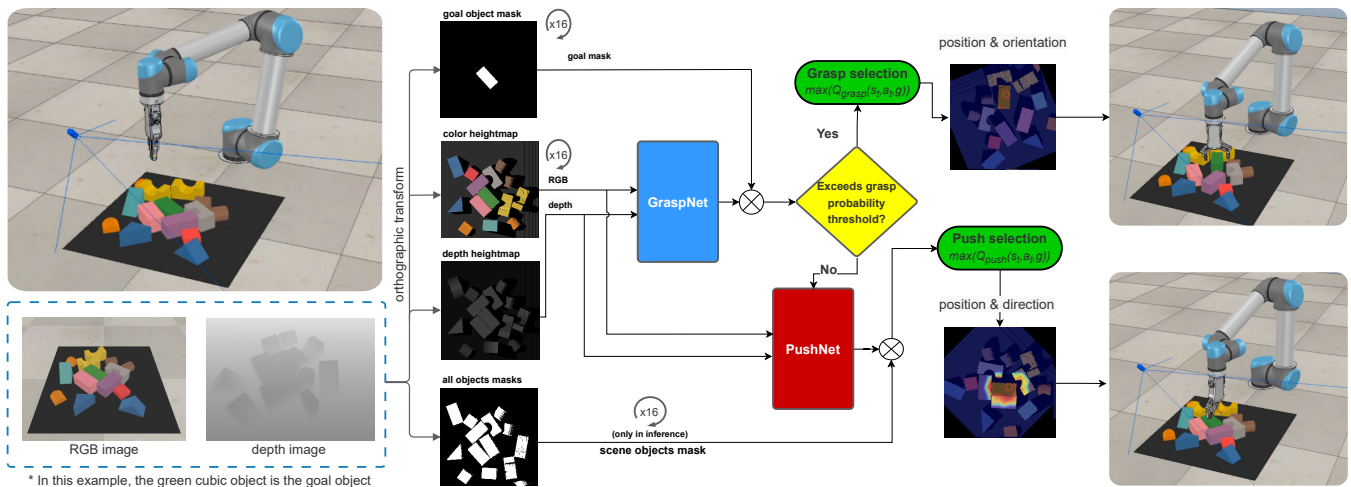


Fig. 2. **Overview** of the entire system. RGB-D camera and UR5 robot arm in CoppeliaSim simulation environment. The camera sensory data undergoes orthographic transformation, and the goal and all objects mask are generated. The color heightmap, depth heightmap, and goal mask are fed into the Grasp net and the push net, all of which experience 16 rotation steps, covering 360 degrees rotation rotating clockwise and starting at 0 degrees. The models produced pixel-wise Q values are considered whether to push or grasp and eventually execute the action. In the testing phase, the all objects mask is used.

the proposed approach in both packed (structured) and pile (unstructured and complicated) scenarios. Experimental results show that the proposed method outperformed the current state-of-the-art approaches by a large margin regarding task completion rate, and grasp success rate (see Sec. IV).

- To the benefit of research communities, we release the source code and the trained models, making it possible to reproduce our results¹.

II. RELATED WORK

This section will mainly cover two fundamental vital aspects of the problem we are tackling, the object grasping problem and the pre-grasp manipulation.

A. Grasping

Autonomous grasping is a challenging problem that has undergone enormous improvement in recent years, especially with Artificial Intelligence (AI) practical approaches. However, robots' dexterity in grasping is one of the most primitive manipulations that allow robots to operate further complex tasks [9]. Classical approaches rely on a model-based approach, where pre-knowledge of the object model is used to estimate force closures and grasp orientation. These methods impose limitations, as it is essential to have accurate modeling of the objects, and that is not always possible [10].

A mathematical model describing objects is crucial to predict the physics of the hand and the grasped object. Various conditions arise during grasping, which is essential to be expressed by the model to achieve stable behavior resisting the different loading conditions [11].

The substantial increase in computing power has allowed the deep-learning methods to prevail in solving the issue. It is focused on data-driven methodology; the data are perceived

in the form of image and depth information of the scene. Then in a simulation setting, the robot exploits the learned visual features to perform a grasp action. The advantage of such an approach is that it does not require explicit knowledge of the objects compared to the classic approaches, i.e., model-based [9]. State-of-the-art and leading work that uses observed geometry to evaluate antipodal grasp pose [12] [13], has sparked enormous interest in the deep learning approach. Inspired by the efficient framework, many studies have taken different approaches in representing the data around the deep learning model, or different models have been used, i.e., Generative Residual Convolutional Neural Network (GR-ConvNet) as model [14]. Another example is research work that generates multi-view 3D object grasping, where objects are represented in the orthographic representation of the depth image from three virtual orthographic views representing the object. After one of the views is selected, it is fed to an auto-encoder that produces a heat-map for a grasp configuration selection [15].

B. Pre-grasp manipulation

RL is widely-used when there is a demand on a cognitive capability [16], i.e., approaching a goal object taking into consideration other objects that are present in the environment. This field of occluded environments has not been studied much, and most studies concerns bin picking (all objects are picked from one bin and placed in another) [2]. Little work is done about having a goal object in a cluttered scene, and a robot arm is attempting to grasp it, which is a fundamental trait for a service robot. This requires efficient pre-manipulation of other objects to be able to grasp the goal object.

Introducing Markov Decision Process (MDP) with a state-space the scene, action space, transition distribution, and reward functions are elements for the RL approach. RL is bound to data consumption, and a time-dependent task

¹<https://github.com/Kamalnl92/Self-Supervised-Learning-for-pushing-and-grasping>

introduces the problem of spars-rewards. The solution to this problem in an MDP setting is to map the current state to action and make the skill of shifting explicitly dependent on the grasping [4].

Most of the former works are top-down grasps; however, that is not sufficient at all times. Especially if the aim is to have safe, stable grasps, it is crucial to include a grasp evaluation of objects in all different orientations. A method that uses reasoning to find an effective grasp sequence to grasp a goal object in a structured clutter uses a cascaded process. By first learning the grasp distribution for a single isolated object and then a discriminate model that captures the collision of the gripper and the present objects in the scene. It is possible to eliminate specific unattainable grasps. The Variation Autoencoder (VAE) is used to evaluate the grasp distribution of the segmented point cloud of the target object as well as the collision check [5].

The synergy between pushing and grasping of objects in clutter remains sample inefficient for the model to receive a reward only after the goal object is grasped. To mitigate the issue, we relabel the goal object, also known as Hindsight Experience Replay (HER) [17]. It contributes to enriching the replay buffer and, in turn, faster learning. We used Xu et al. [3] as a starting point for our project. Thus, it will be explained in more detail. The modeling synergy of the push-grasping goal-oriented problem as Markov Decision Process (MDP) enriches the concept of model decision making in some parts of it are random and others under control. For the process of pushing and grasping, there are many reasons that action previously succeeded in execution will not work in current or future attempts due to simulation physics inconsistency. These factors are challenging to be all capture if the model requires total dependence on it. The approach of using Visual Pushing for Grasping (VPG) coined by [2] gives the system the flexibility of less relying on the physics of the simulation environment. As it learns to cope with it from experience. The push action is landing the robot arm on desired coordinates then performing pushing action in one selected direction from the 16 directions. Moreover, grasping in a similar strategy, with respect to the orientation of the object grasping is performed.

III. METHOD

This section discusses the overall system architecture, the grasp and the push models hierarchical framework, and the training procedure in detail.

A. Overall system

As shown in Fig. 2, the system produces two actions, push or grasp, depending on what is feasible in the environment. Grasping the goal object is executed when the likelihood of grasping the goal object exceeds the threshold. Otherwise, the goal object or its surrounding objects are pushed approximately 1.3cm away from the current position to increase the probability of grasping the goal object successfully. The grasp/push points and direction are indicated on the image

coordinate (output of the networks) and then transformed to the robot’s reference frame to be executed.

The policy is represented as $\pi(s_t|g)$, the reward as $R(s_t, a_t, g)$, and lastly the Q -value function as $Q(s_t, a_t, g)$. Pushing and grasping in an occluded environment is formulated in a reinforcement learning setting. The camera data of the working scene is transformed into orthographic images and rotated 16 times to cover 360 degrees rotation. The rotations are approximately 22.5 degrees increase for each step. The rotation allows the models to express and learn grasp orientation and push direction. The model maximum Q -value is selected with respect to the rotation, and then action is executed. If the grasp threshold exceeds a certain Q -value (we set it to 1.8), a grasp action to the goal object is executed. Else, push of the goal object or any other objects is performed [3].

The pushing is performed in a manner that increases the probability of successfully grasping the goal object in the future. Similar to what we would have in Generative Adversarial Network (GAN), the grasp net ϕ_g serves as a discriminator, and the push net ϕ_p is considered a generator. It manipulates the scene to utilize an increase in the grasp Q -value, particularly the Q_g (see Fig. 2). The discrete mask of the goal object is used both as input in the model and as output to remove irrelevant pixel Q -values.

Unlike to [3], the mask of all objects is not clear when it is used. We decided during training not to restrict the model to have the Q -values only on the relevant objects. It enhances the exploration space of the model due to considering all Q -values and executing at the max value. Nevertheless, we used the objects mask at the output during inference.

The discrete masking proposed by [3] is not useful as it consistently results in invalid actions (see Fig. 3 *top-row*). Having pixel-wise Q -values at no objects leads to useless grasping and pushing actions. Wrong orientation grasps and pushes direction is performed. Referring back to Fig. 3, in the right-most top corner, there is a red circle, which is the max pixel-wise Q -value, consequently, undesirable action is executed. Moreover, their approach requires different masking during the training and testing phases; it impacts the scalability of the system. More advanced instance segmentation methods (e.g., [18]) can be used to cope with this problem. However, since the perception is out of the scope of this paper, we simplify the problem by using RGB-colors segmentation as we know the color of the goal object in advance (i.e., green color). The working discrete mask after applying it to the pixel Q -values is illustrated in Fig. 3 (*lower-row*).

B. Models hierarchical framework

The hierarchical framework consists of two networks (grasp ϕ_g and push ϕ_p) sharing the same structure. Unlike to Xu et al. [3] We use two 121-layer DenseNets [8], pre-trained on ImageNet [19], to extract visual features. Our system is 1/3 smaller than [3] The first DenseNet tower takes the RGB data of the scene, the second one takes the normalized depth image. The output of these networks is then concatenated

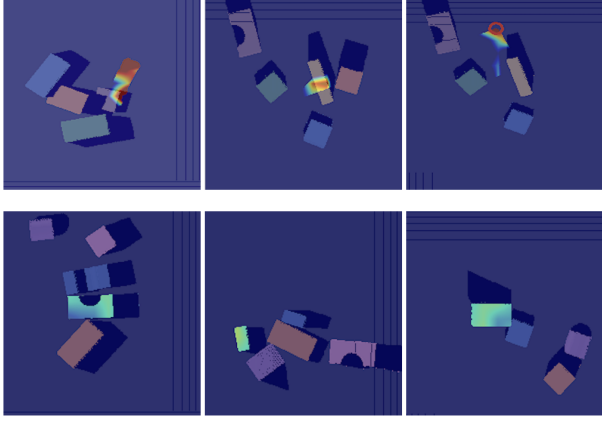


Fig. 3. Objects pixels Q -value after applying masking: (*top-row*) masking problems in approach proposed by [3]; (*lower-row*) Accurate masking using our method.

to form a single feature vector for the given observation. The obtained representation is fed into a fully convolutions network [20], which contains two Kernels of 1×1 and Rectified Linear Unit (ReLU) activation function, and batch normalization [21]. Finally, it is bilinearly upsampled to generate a pixel-wise prediction (i.e., the output image will be the same size as the input cropped image).

C. Models training

We train the model in three sequential stages: the first stage is training the goal-condition grasping, the second stage is dedicated to goal-conditioned pushing, and lastly, alternating the training between the goal-condition grasp and push. The grasp reward R_g and push reward R_p , are formulated as follows:

$$R_g = \begin{cases} 1, & \text{if grasp success} \\ 0, & \text{if not} \end{cases} \quad (1)$$

$$R_p = \begin{cases} 0.5, & Q_g^{improved} > 0.1 \ \& \ \text{scene change} \\ -0.5, & \text{no scene change} \\ 0, & \text{otherwise} \end{cases} \quad (2)$$

where $Q_g^{improved}$ is calculated as

$$Q_g^{improved} = Q_g^{post-push} - Q_g^{pre-push} \quad (3)$$

Furthermore, the amount of changes in the scene is calculated from the depth map surrounding the goal object. Inspired by the Bellman equation of RL, we can formulate the state action function with respect to the goal object as $\pi(s|a, g)$. We use the epsilon-greedy action selection strategy $\epsilon(\pi(s|a, g))$. It gives the agent the privilege to both explore and exploit options [22]:

$$\nu(S_t, g) = E[R_{[t+1]} + \rho\nu(S_{[t+1]})|S_t = S, g] \quad (4)$$

Where ρ represents a discount function, an overview of the training process and the grasp success rate for the different stages of training are depicted in Fig. 5. In the following sub-sections, more details about the training are discussed.

1) *Goal-conditioned grasping*: To train the model, we randomly generate sparse scenes by putting five objects in the workspace (e.g., see Fig. 3). In this stage, we consider the execution of each grasp as an episode and train the model in two phases. The first phase, i.e., *grasp agnostic*, is done by relabeling the goal object to increase the sample efficiency. In the second phase, i.e., *grasp explore* as the model learned to grasp objects, we assume it learned sufficient estimation of the orientations and grasp pose; hence, we omit the relabeling of the goal-object. In both phases, the ϵ -greedy strategy is used for balancing the trade-off between exploring and exploiting [23]. Unlike what has been used by [3] which measures the Q -values to determine when to stop training, we measure the grasp success rate directly. Figure 5 shows that the training could be stopped in both phases after reaching 1400 grasp epochs since the model grasp success is mostly stable. Even though the grasp success does not increase much in the grasp explore phase, the task is more challenging as only the goal object grasp is considered a success, and the environment might not have a feasible grasp due to yet untrained push model.

2) *Goal-conditioned pushing*: In this round of training, we fix the grasp model and only train the push model based on adversarial training, as mentioned earlier. Each episode has been defined as up to five pushes and a grasp in the end. In other words, if the Q -value of the grasp for the goal object exceeds a given threshold, the robot immediately executes the grasp action, and the episode is terminated. After a short period of 120 training grasp epochs, we observed that the goal-oriented grasp success rate increases dramatically as the push model manipulates the scene. Consequently, it increases the probability of the goal object's grasp (see Fig. 5 *third-row*). A positive reward is given to the push model only if it increases the future probability of grasping the goal object.

3) *Goal-conditioned alternating*: In the previous grasping stage, we trained the grasp model in sparse environments (i.e., around five objects per scene) to reduce the effect of occlusion. In addition, the model was trained when the push was not trained yet, which leads to the distribution mismatch problem. The grasp net is further trained after the push model is trained to overcome this issue. Models are alternately trained in an environment with ten objects present in the scene to improve the synergy between the grasp and push models.

Illustration of the training process is depicted in Fig. 5. Since the grasping success result is a binary result (i.e., 1 success and 0 for a failure), we use exponential smoothing with a factor of 0.9 to show trends in the data, i.e., learning progress of the grasp success. Also, the averaging mean is used to show the data variation. For the goal-condition grasping and goal-conditioned pushing, we use the mean rolling window of size 50, and the rest we set to mean of 7.

Pushing objects is not legible for all objects in the scene. In addition, the model's realization of all variations of friction values is challenging. There are objects such as bottles or cereal boxes that pushing actions up on them from a top-down approach would cause chaos. We developed another

strategy to perform a grasp of non-goal objects to be able to perform clearing around the goal object and contribute to a future goal grasp. The model should perform a sequence of grasp actions to non-goal objects until a state where grasping the goal object is possible.

We aim to avoid chaos in the scene. Having the first push actions to reach the goal object would not work in this case. Force trying to grasp objects would lead to objects being toppled on the working floor and unable to grasp anymore. In our approach, we introduce objects that can be found in a household, with closely related sizes, height length of 17cm and a minimum length of 3cm —the width and thickness have different variations. An example of such a scenario is depicted in Fig. 4, the green object is the goal object. Due to the presence of the adjacent objects, the robot arm would collide with other objects. One needs to examine the motion pattern while training. Using a non-responsive robot arm colored green would examine a motion plan if it is collision-free and act accordingly. The orientation needs to be more accurate than the previous approaches (pushing to clear the goal object from obstacles). In the previous approach, even when the grasping is not nicely estimated but close enough, the object would comply and rotate slightly due to the up-down force of the gripper and slide into the antipodal gripper. The latter will not be possible with the grasp removing non-goal objects. There would be a risk of objects falling on the working floor, which we want to avoid. For the goal object, we introduce projection of the pixel-wise Q-values to estimate the location and the orientation composed of the accumulation of all Q-values. Unlike the previous approach, where we rely on multiple predictions, which is quite a common approach in machine learning, providing a more stable estimation. By taking the max accumulated value collectively for each rotating heightmap, orientation is selected. Then the projection median values are used to determine the location.

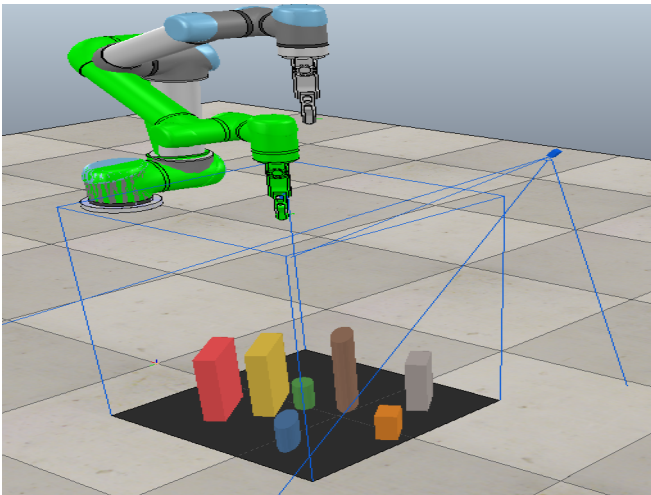


Fig. 4. Setup in CoppeliaSim simulation environment using the strategy of grasping to remove objects. Two robot arms, one physically responsive, the other robot arm with the color green, is not physically responsive.

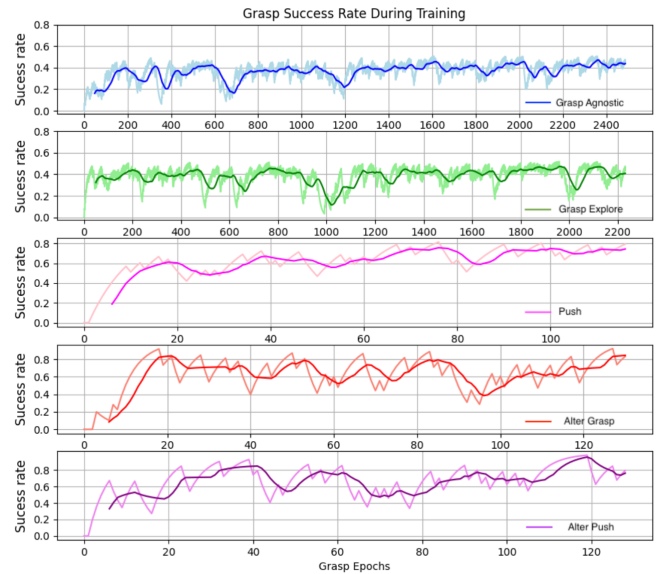


Fig. 5. Grasp success rate versus number of grasp epochs. The top two are related to the grasping network ϕ_g training, the middle one for the push network ϕ_p training. The last two are when the training is alternated between the grasp net and push net.

The problem of grasping and removing objects is more complex compared to the push to grasp. We deal with delicate grasping and sequence of removing objects. After training the model, we encountered irregularity (non-linear in relation to the amount of conclusion around the goal object) with an occupation ratio around the goal object, which does not work well with higher objects. The thresholds for grasping and pushing have also been manipulated so that in the push training stage, the grasp non-goal model would have the chance to perform. However, the model has not converged, and the grasp completion stayed around 40%. This approach is not working for such cases. The consistent collision of the robot arm with objects in the scene and the sequence decoding of removing collision objects seem impossible for the model to learn. Approaches such as curriculum learning could mitigate the issue [24]. It addresses a complex problem where a sequence of tasks is presented with an increase in difficulty.

IV. EXPERIMENT

To evaluate the proposed approach, we carried out extensive sets of experiments in the CoppeliaSim simulation environment [25]. Our experimental setup consists of a UR5 robot arm and RGB-D Intel RealSense SR300, as shown in Fig. 2. We used inverse kinematics (IK) solver for motion planning purposes [26]. The networks are trained with Adam optimizer [27], the learning rate is fixed on 10^{-4} , and weight decay of 2^{-4} has been considered. We trained the models using NVIDIA V100 Graphics Processing Unit for faster training time. We compare our approach to Xu et al. [3] since, to the best of our knowledge, it is the current state-of-the-art approach in the domain of goal object oriented that handles such scenarios. We train and test both approaches on

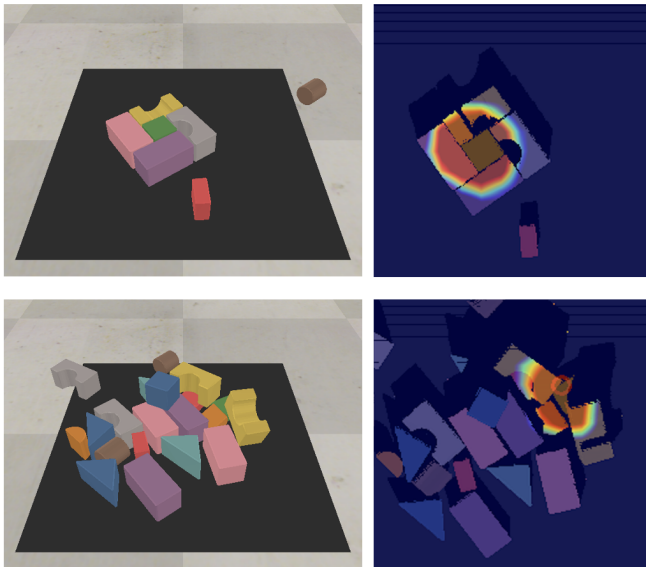


Fig. 6. Two examples of the generated scene are packed and pile scenarios for evaluation purposes. In all experiments, the goal object is defined by green color: (*top-row*) an example of packed scene (structured) and its heat-maps (pixel Q -values); (*bottom-row*) an example of an unstructured scene (pile) and its heat-maps (pixel Q -values).

the same hardware and same evaluation scenes to achieve fair comparison. We use the following evaluation metrics that have been used previously by [2], [3]:

- **Completion (C):** The mean percentage completion over n test runs. Completions are successful and equal to 1 in a test run; if the system does not exceed in failing to grasp the goal object $n = 5$ times, else it is 0. The metric measures the system’s ability to complete the task.
- **Grasp success (GS):** The mean percentage of successful grasp over all grasp attempts. This metric represents the accuracy of the model and its ability to estimate goal object successful grasp.
- **Motion number (MN):** The mean number of push actions per completion. It reflects action efficiency.

To evaluate the proposed approach, we conducted two sets of experiments. One is a packed (structured) scenario, and the other is a pile (unstructured and complicated) scenario. In the first round of experiments, we evaluate the system’s consistency by performing the same experiment 100 times in a packed scenario. An example scene of this experiment together with its heat-maps (pixel-wise Q -values) are depicted in Fig. 6 (*top-row*). The obtained results are summarized in Table I. The low standard error values indicate that our approach produces a consistent sequence of actions to accomplish the task successfully. Furthermore, we

TABLE I

SIMULATION CONSISTENCY RESULTS ON STRUCTURED SCENE

Approach	C%	GS%	MN
Xu et al. [3]	83.0 ± 3.75	26.48 ± 2.16	3.43 ± 0.31
Ours	98.98 ± 1.01	86.08 ± 3.32	1.12 ± 0.03

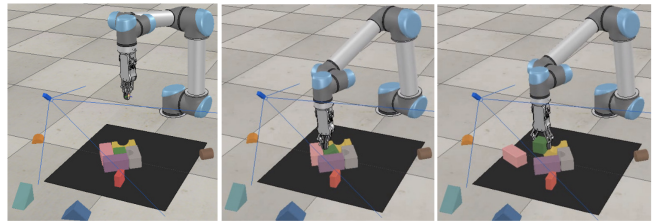


Fig. 7. Sequence of snapshots showing the robot performing decluttering by pushing the objects surrounding the target object to make grasping the goal object feasible: (*left*) initial scene; (*middle*) pushing surrounding objects; (*right*) grasping the goal object.

observed that the model strives to gain a push reward (see Eq. 2). Hence, pushing the goal object frees it quickly from obstacles. The Q -values are high in value on and around the goal object. Therefore, shifting the goal object facilitates free space around the target object to be grasped (see Fig. 7). By looking at representative scenarios of Fig. 6, we hypothesize that approximately one push to grasp the goal object is highly efficient.

In the first experiment, our approach achieves a 99% completion rate (C), which is 16% better than Xu et al. [3]. Also, in terms of Grasp Success (GS), our proposed approach shows ($\approx 60\%$) better performance. Xu et al. [3] approach, the robot tends to perform unsuccessful grasps of the target object as it lacks the proper estimation of the space around the goal object, mainly due to the poor masking during both training and inference. It led to several consecutive failures and the termination of the experiment. Our model has better accuracy in making feasible grasp estimations. It has learned to pick up the target object with a remarkably higher grasp success rate.

In the second set of tests, we assess the performance of the proposed approach by generating random scenes using 10, 15, and 20 objects.

It is worth mentioning that having more objects in the scene makes the task more complicated. For these experiments, we drop different primitive objects in the scene sequentially from a pre-defined point in the middle and above the working scene to generate test scenes randomly. It results in more dense scenarios, and the goal object gets covered by other objects in some instances (see Fig. 8 *left*). We selected a goal object for each experiment out of the possible primitive set of objects. An example of such scenes is depicted on the *bottom-row* of Fig. 6. We evaluate the proposed approach by generating 100 different scenes for each level of complexity (i.e., 10, 15, 20 objects per scene). The obtained results are presented in Table II.

We hypothesize that the goal mask input to the model is not useful. The power of such models is to learn the non-linearity of the data. Discrete inputs are not beneficial. It is clear that there is a substantial amount of pixel-wise Q -values at no objects, which could lead to necessary push/grasp actions, hence the importance of the output mask. To validate the goal mask as an input to the model, we train and test the model with a mask as an input and another without. In table II, we see the values completion rate (C) and

Grasp Success (GS) are insignificantly different. The motion number, on average, is higher with a 1 motion move. We think it is acceptable knowing it is a 1/3 smaller model.

Across the completion metric and grasp success rate, we see that our system performed significantly better. However, regarding the Motion Number metric, our system scored lower. On average, we observed that in scenes containing 10 objects, one push action was highly efficient in completing the task.

By increasing the level of complexity (adding more objects to the scene), we expected the model to score lower across all metrics since the model has never encountered a scene containing more than 10 objects during the training phase. When we tested the agent with 15 objects per scene, we observed that the agent performed better in terms of task completion and grasp success rate. On a closer inspection, we found that even though there are more objects in the scene, in some instances, the goal object was pushed away and became isolated after other objects were spawned into the scene (see Fig. 8 *middle*). Such situations made grasping the goal object easier. By increasing the number of objects to 20, such cases occurred rarely, and complicated scenes were often generated, as depicted in Fig. 8 *right*). Therefore, as we expected, the performance of both approaches decreased. By comparing obtained results, it is visible that the proposed approach outperformed Xu et al. [3] regarding task completion and grasp success rate. With 20 objects in the scene, our system completed the task with at least 97.22 ± 1.95 which is approximately 20% (on average) better than Xu et al. [3] performance.

Another interesting point is that, however, the proposed system performed well regarding task completion and grasp success rate metrics. It showed a higher MN than Xu et al. [3]. As this metric reflects action efficiency, one wants to aim for lower values. Since Xu et al. [3] model makes the wrong estimation of a feasible goal object grasp, we observed that it keeps attempting to grasp the goal object even when it is not feasible at all. Attempting to grasp the goal object results in moving objects in the scene, and this action is not counted in the MN metric (as MN is defined as the number of push actions per completion). Therefore, Xu et al. [3] model showed a better MN performance. Nevertheless, not in a desirable manner, it is not systematical to avoid pushing though it is essential, it loses the purpose of synergy value between the push and the grasp action. Our grasp success rate might be on the low spectrum, but this can be improved by increasing the grasp probability threshold. However, that will cause a decrease in the push efficiency as the model will make more pushes and improve clearing to the degree that it has higher grasp probability confidence. Overall, our system showed consistent performance despite the increased number of objects.

V. CONCLUSION AND FUTURE WORK

This paper presents a self-supervised deep RL approach enabling a robot to grasp a goal object by pushing other objects away when needed. We trained and tested the model

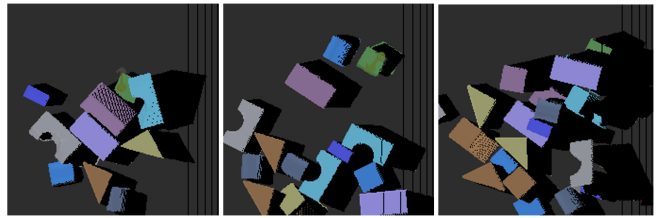


Fig. 8. Typical scenes with different number of present objects, starting from left to right 10, 15, and 20 respectively.

TABLE II
SIMULATION RESULTS ON 100 DIFFERENT COMPLICATED SCENES

Approach	#objects	C%	GS%	MN
Xu et al. [3]	10	71.56 ± 4.48	20.35 ± 1.57	0.64 ± 0.25
Xu et al. [3]	15	71.0 ± 4.56	22.72 ± 1.75	1.1 ± 0.54
Xu et al. [3]	20	77.89 ± 4.27	21.59 ± 1.78	1.13 ± 0.45
Ours (mask)	10	98.97 ± 1.02	66.21 ± 3.91	1.02 ± 0.14
Ours (mask)	15	100 ± 0.0	74.60 ± 3.89	3.67 ± 0.98
Ours (mask)	20	97.22 ± 1.95	69.23 ± 4.62	6.09 ± 1.82
Ours (no mask)	10	98.78 ± 1.22	68.33 ± 4.29	3.19 ± 0.56
Ours (no mask)	15	100 ± 0.0	71.42 ± 4.28	3.27 ± 0.47
Ours (no mask)	20	99.22 ± 0.1	67.36 ± 4.83	7.12 ± 2.04

in two challenging scenarios: packed objects and a pile of objects. We illustrated that previous work is not reproducible as claimed results by testing with objects in a packed scenario where the objects are tightly packed together and form a structured scene, while in the pile scenario, we randomly dropped up to 20 objects inside the robot’s workspace to make a complicated and unstructured scene. Experimental results proved that the proposed approach enabled the robot to interact robustly with the environment and successfully manipulate the goal object in both scenarios. Our system outperformed the selected state-of-the-art in terms of task completion rate and grasp success in both scenarios. In the case of MN metric, our approach outperformed Xu et al. in the packed scenario, while Xu et al. worked better than ours in the pile scenario.

The pushing strategy has some limitations for objects that are hard to push due to friction with the surface under the object or causing objects to fall from their standing positions. In real-life settings, this limitation can cause problems as the robot is often confronted with various levels of friction. Undoubtedly, for objects that have three times the heights of the object that we used in the push testing, shifting them will cause the object to be laid on the surface. Thus, we trained and tested the model to use the approach of grasp removing the non-goal objects. It is too complex for the current architecture to learn, but curriculum learning could be a possibility. In the continuation of this work, we would like to investigate further the possibility of grasp removing non-goal objects in the future.

ACKNOWLEDGMENT

We thank the Center for Information Technology of the University of Groningen for their support and for providing access to the Peregrine high-performance computing cluster.

REFERENCES

- [1] T. Kunz, U. Reiser, M. Stilman, and A. Verl, "Real-time path planning for a robot arm in changing environments," in *2010 IEEE/RSJ International Conference on Intelligent Robots and Systems*. IEEE, 2010, pp. 5906–5911.
- [2] M. Fujita, Y. Domae, A. Noda, G. Garcia Ricardez, T. Nagatani, A. Zeng, S. Song, A. Rodriguez, A. Causo, I.-M. Chen *et al.*, "What are the important technologies for bin picking? technology analysis of robots in competitions based on a set of performance metrics," *Advanced Robotics*, vol. 34, no. 7-8, pp. 560–574, 2020.
- [3] K. Xu, H. Yu, Q. Lai, Y. Wang, and R. Xiong, "Efficient learning of goal-oriented push-grasping synergy in clutter," *IEEE Robotics and Automation Letters*, vol. 6, no. 4, pp. 6337–6344, 2021.
- [4] L. Berscheid, P. Meißner, and T. Kröger, "Robot learning of shifting objects for grasping in cluttered environments," in *2019 IEEE/RSJ International Conference on Intelligent Robots and Systems (IROS)*. IEEE, 2019, pp. 612–618.
- [5] A. Murali, A. Mousavian, C. Eppner, C. Paxton, and D. Fox, "6-dof grasping for target-driven object manipulation in clutter," in *2020 IEEE International Conference on Robotics and Automation (ICRA)*. IEEE, 2020, pp. 6232–6238.
- [6] B. Tang, M. Corsaro, G. Konidaris, S. Nikolaidis, and S. Tellex, "Learning collaborative pushing and grasping policies in dense clutter," in *2021 IEEE International Conference on Robotics and Automation (ICRA)*. IEEE, 2021, pp. 6177–6184.
- [7] Y. Yang, H. Liang, and C. Choi, "A deep learning approach to grasping the invisible," *IEEE Robotics and Automation Letters*, vol. 5, no. 2, pp. 2232–2239, 2020.
- [8] G. Huang, Z. Liu, L. Van Der Maaten, and K. Q. Weinberger, "Densely connected convolutional networks," in *Proceedings of the IEEE conference on computer vision and pattern recognition*, 2017, pp. 4700–4708.
- [9] H. Duan, P. Wang, Y. Huang, G. Xu, W. Wei, and X. Shen, "Robotics dexterous grasping: The methods based on point cloud and deep learning," *Frontiers in Neurorobotics*, vol. 15, p. 73, 2021.
- [10] A. Sahbani, S. El-Khoury, and P. Bidaud, "An overview of 3d object grasp synthesis algorithms," *Robotics and Autonomous Systems*, vol. 60, no. 3, pp. 326–336, 2012.
- [11] D. Prattichizzo and J. C. Trinkle, "Grasping," in *Springer handbook of robotics*. Springer, 2016, pp. 955–988.
- [12] A. t. Pas and R. Platt, "Using geometry to detect grasps in 3d point clouds," *arXiv preprint arXiv:1501.03100*, 2015.
- [13] A. ten Pas, M. Gualtieri, K. Saenko, and R. Platt, "Grasp pose detection in point clouds," *The International Journal of Robotics Research*, vol. 36, no. 13-14, pp. 1455–1473, 2017.
- [14] S. Kumra, S. Joshi, and F. Sahin, "Antipodal robotic grasping using generative residual convolutional neural network," in *2020 IEEE/RSJ International Conference on Intelligent Robots and Systems (IROS)*. IEEE, 2020, pp. 9626–9633.
- [15] H. Kasaei and M. Kasaei, "Mvgrasp: Real-time multi-view 3d object grasping in highly cluttered environments," *arXiv preprint arXiv:2103.10997*, 2021.
- [16] M. Q. Mohammed, K. L. Chung, and C. S. Chyi, "Review of deep reinforcement learning-based object grasping: Techniques, open challenges, and recommendations," *IEEE Access*, vol. 8, pp. 178 450–178 481, 2020.
- [17] M. Andrychowicz, F. Wolski, A. Ray, J. Schneider, R. Fong, P. Welinder, B. McGrew, J. Tobin, O. Pieter Abbeel, and W. Zaremba, "Hindsight experience replay," *Advances in neural information processing systems*, vol. 30, 2017.
- [18] Y. Xiang, C. Xie, A. Mousavian, and D. Fox, "Learning RGB-D feature embeddings for unseen object instance segmentation," in *Conference on Robot Learning (CoRL)*, 2020.
- [19] J. Deng, W. Dong, R. Socher, L.-J. Li, K. Li, and L. Fei-Fei, "Imagenet: A large-scale hierarchical image database," in *2009 IEEE conference on computer vision and pattern recognition*. Ieee, 2009, pp. 248–255.
- [20] J. Long, E. Shelhamer, and T. Darrell, "Fully convolutional networks for semantic segmentation," in *Proceedings of the IEEE conference on computer vision and pattern recognition*, 2015, pp. 3431–3440.
- [21] S. Ioffe and C. Szegedy, "Batch normalization: Accelerating deep network training by reducing internal covariate shift," in *International conference on machine learning*. PMLR, 2015, pp. 448–456.
- [22] M. Gimelfarb, S. Sanner, and C.-G. Lee, "{\epsilon}-bmc: A bayesian ensemble approach to epsilon-greedy exploration in model-free reinforcement learning," *arXiv preprint arXiv:2007.00869*, 2020.
- [23] C. D'Eramo, A. Cini, and M. Restelli, "Exploiting action-value uncertainty to drive exploration in reinforcement learning," in *2019 International Joint Conference on Neural Networks (IJCNN)*. IEEE, 2019, pp. 1–8.
- [24] S. Narvekar, B. Peng, M. Leonetti, J. Sinapov, M. E. Taylor, and P. Stone, "Curriculum learning for reinforcement learning domains: A framework and survey," *arXiv preprint arXiv:2003.04960*, 2020.
- [25] E. Rohmer, S. P. N. Singh, and M. Freese, "V-rep: A versatile and scalable robot simulation framework," in *2013 IEEE/RSJ International Conference on Intelligent Robots and Systems*, 2013, pp. 1321–1326.
- [26] R. Diankov, "Automated construction of robotic manipulation programs," 2010.
- [27] D. P. Kingma and J. Ba, "Adam: A method for stochastic optimization," *arXiv preprint arXiv:1412.6980*, 2014.